



Contents lists available at ScienceDirect

Journal of the Mechanical Behavior of Biomedical Materials

journal homepage: www.elsevier.com/locate/jmbbm

Shear thinning/self-healing hydrogel based on natural polymers with secondary photocrosslinking for biomedical applications

Esmat Jalalvandi^{a,*}, Amin Shavandi^b^a Department of Mechanical Engineering, College of Engineering and Mathematical Sciences, University of Vermont, Burlington, VT 05405, USA^b Centre for Bioengineering and Nanomedicine, Department of Food Science, University of Otago, Dunedin 9054, New Zealand

ARTICLE INFO

Keywords:

Hydrogel
Guest-host chemistry
Self-healing
Photocrosslinking

ABSTRACT

Injectable hydrogel systems are useful in many biomedical applications, including drug or cell delivery carriers and scaffolds. Here, we describe the design and characterization of a shear thinning hydrogel that undergoes a disassembly when shear forces are applied during injection and is self-healing once the shear forces are removed. This hydrogel is based on a cyclodextrin modified alginate, and a methacrylated gelatin which initially forms through a weak guest-host interaction between hydrophobic cyclodextrin cavities and the aromatic residue of gelatin. Methacrylated gelatin possesses photocrosslinkable functionalities which can go through a light-initiated polymerization to create secondary crosslinking sites and further crosslink the matrix. The shear thinning and self-healing behavior of these gels monitored in low and high strain range, viscosity of the hydrogels components and gelation kinetic were studied. The rheological analyses showed the formation of shear thinning gels which were further stabilized by visible light exposure. The cytotoxicity of the hydrogels towards human mesenchymal stem cells were assessed and the rate of mass loss over a week period was studied.

1. Introduction

Hydrogels are 3-D crosslinked matrices that can absorb and retain significant amount of water. These networks are crosslinked physically and/or chemically and are employed in various biomedical applications such as drug or cell delivery, tissue engineering, cell microenvironment engineering, wound dressing and sealants (Jalalvandi et al., 2018; Huang et al., 2017). Of various types of crosslinking methods, injectable hydrogels are particularly interesting for clinical use. These hydrogels are applied through a syringe and undergo a sol-gel transition at the site of injection where they can fit the geometry of target site, through a minimally invasive procedure (Jalalvandi et al., 2016).

For many injectable systems, payload and polymer solutions are presented to the injection site in a liquid form and polymerized *in situ* using chemical crosslinkers, changes in temperature, pH or ionic strength (Ma et al., 2017; Teodorescu et al., 2015). Despite the increasing development of injectable hydrogels, these systems face some limitations. For instance, if gelation occurs slowly, it might cause leakage of the precursors and loss of payload in delivery applications before gel formation whereas very fast gelation may result in delivery failure as well as complication in surgical applications (Feng et al., 2016; Qin et al., 2017). Preferably, shear thinning hydrogels with pseudoplastic behavior will not show these issues related to kinetic as

they constantly flow under shear stress and re-assemble once the shear stress is stopped (Guvendiren et al., 2012). Shear thinning hydrogels are considered injectable matrices that form through reversible physical interactions in mild conditions. The crosslinking method of shear thinning materials does not require chemical reaction and is mostly based on dynamic and inherently weak physical interactions such as hydrophobic interactions (Yan et al., 2010), guest-host interactions (Appel et al., 2014), hydrogen bonding (Dankers et al., 2012) and electrostatic interactions (Ding et al., 2016). These dynamic materials disassemble when subjected to shear stress and recover or self-repair once the shear force is removed (Loebel et al., 2017; Qiang et al., 2015). The recovery characteristics is beneficial at the injection site (Lee et al., 2009) especially for targets that are under mechanical stress such as nucleus pulposus, or those that undergo constant dynamic motion such as cardiac tissue (Rodell et al., 2015).

Nevertheless, the shear thinning/self-healing materials are usually limited by their low mechanical strength and fast degradation time depending on the crosslinking groups and their affinity (Guvendiren et al., 2012; Appel et al., 2012). The relatively unstable nature of these networks restrains their ability as prolonged therapeutic delivery system and tissue engineering scaffolds. To overcome these limitations, addition of a secondary crosslinking technique have been explored to introduce more stability to the shear thinning hydrogels (Rodell et al.,

* Corresponding author.

E-mail address: e.jalalvandi@hw.ac.uk (E. Jalalvandi).<https://doi.org/10.1016/j.jmbbm.2018.10.009>

Received 31 July 2018; Received in revised form 1 October 2018; Accepted 3 October 2018

Available online 12 October 2018

1751-6161/ © 2018 Elsevier Ltd. All rights reserved.

2015; Lu et al., 2013). For example, photocrosslinking results in covalent linkages between interacting polymer chains to form polymeric networks. Both ultraviolet (UV) and visible light sources have been employed to initiate crosslinking; however, UV exposure may result in adverse effect on some cellular activities for *in vivo* applications if the intensity of the light is not controlled accurately (Fedorovich et al., 2009). During the crosslinking process using UV, the energy of the polymerizing light, heat, and/or free radical species may cause cellular necrosis, and tissue damage. This limits the use of hydrogels as drug or cell carriers (Bryant et al., 2000; Baroli, 2006). As a safe alternative to UV exposure, the use of visible light with less harmful effects has been investigated (Hao et al., 2014).

In current study, a shear thinning hydrogel based on guest-host interactions is presented which was further crosslinked through a secondary chemical crosslinking to stabilize the system. This network is composed of biodegradable and biocompatible polymers (gelatin and alginate) which is advantageous for the use in biomedical applications (Schexneider, 2004; Manjula et al., 2013). Gelatin is a natural macromolecule that has been used in pharmaceuticals, cosmetics and food industry (Su and Wang, 2015). It is processed by denaturation of collagen and its amino-acid composition is similar to that of collagen molecules such as tryptophan phenylalanine and tyrosine (Duconseille et al., 2015). Gelatin can be modified chemically using methacrylic anhydride to impart a functional group capable of covalent crosslinking (Wang et al., 2017; Arya et al., 2016). Alginate is a natural polysaccharide used in wide range of biomedical applications due to its biocompatibility and biodegradability (Szekalska et al., 2016; Kim et al., 2011). Carboxylic groups of alginate can be coupled with amine groups through a carbodiimide-mediated amidation (Chhatbar et al., 2012). β -cyclodextrin (CD) is a naturally occurring cyclic oligosaccharides composed of seven β -glucose units with a central hydrophobic cavity and hydrophilic exterior surface. In an aqueous solution, water molecules inside the CD cavity can easily be replaced by guest molecules (or part of the molecules), leading to an inclusion complex in a reversible process (Liu and Guo, 2002; Loftsson and Brewster, 1996). Amine-modified CD can be immobilized into alginate backbone through carbodiimide-mediated amidation to create a CD-functionalized alginate with the ability to form weak guest-host interactions with aromatic residues of gelatin (e.g., tryptophan phenylalanine and tyrosine) (Feng et al., 2016; Farris et al., 2010; Ma et al., 2015). We speculate that the complexation between CD and aromatic groups is the main crosslinking mechanism for formation of initial shear thinning hydrogel. For more physically demanding applications, a dual crosslinking mechanism might be preferred to form a matrix with higher mechanical strength and longer degradation period. Herein, a dual crosslinking technique was employed to form hydrogels based on biopolymers. The hydrogels were first assembled through a reversible physical interaction mediated by guest (CD moieties in CD functionalized alginate)-host (aromatic residues of gelatin) interaction. The crosslinking process continued by illumination of visible green light in the presence of photoinitiator to polymerize the photoresponsive vinyl groups on modified gelatin. Secondary crosslinking technique significantly increased the storage moduli of the hydrogels compared to the initial crosslinking method to prepare shear thinning materials. The same effect was observed while studying the *in vivo* degradation time of the hydrogels. Morphology and biocompatibility of single and dual crosslinked hydrogels were also studied to assess their potential application in biomedical area.

2. Experimental section

2.1. Materials

Gelatin from porcine skin, Eosin Y, 1-vinyl-2-pyrrolidinone (VP), triethanolamine (TEA), thiazolyl blue tetrazolium bromide (MTT), methacrylic anhydride, trypsin-EDTA, penicillin-streptomycin, 10% sodium dodecyl sulphate (SDS), 1-ethyl-3-(3-dimethylamino)

carbodiimide hydrochloride salt (EDC), human mesenchymal stem cells (HMSC), dimethyl sulfoxide (DMSO), DCl and D₂O were purchased from Sigma-Aldrich. Sodium alginate (G/M:0.6, 190–240 kDa), and PBS tablets were acquired from MP Biomedicals. β -cyclodextrin (β -CD) was purchased from AK scientific. Fetal bovine serum (FBS) was supplied by Hyclone™. Cell culture media (minimum essential media, MEM, without phenol red) was acquired from Gibco™. Ethylenediamine (EDA), N-hydroxysuccinimide (NHS), L-tyrosine and *p*-toluene sulfonyl chloride were acquired from ACROS Organics.

2.2. Instrumentation

¹H NMR spectra were recorded on a 400 MHz Varian INOVA spectrometer at 298 K in D₂O solvent and were referenced to the internal solvent signals, which chemical shifts reported in ppm units. A relaxation delay of 10 s was used for recording the ¹H NMR spectra. Fourier transform infra-red (FTIR) spectra were recorded on a Bruker optic Alpha-p spectrometer with a diamond Attenuated Total Reflectance (ATR) top-plate. The lyophilization process was carried out on a LABCONCO freeze dry system at -40°C and 8×10^{-6} bar. Rheological characterizations including, viscosity, dynamic shear testing and time sweeps were conducted at 25 and 37 °C using the Haake RS1 rheometer (ThermoFisher, Waltham, MA) with steel cone plate geometry (1° 59' 6" and 20 mm diameter). After mixing the component of each hydrogel in a 5 mL syringe equipped with a 15-gauge needle (nominal outer diameter: 0.072", nominal inner diameter 0.054"), the sample (300 μL) was deposited on the rheometer plate for rheological analyses. The microstructure of the hydrogels was examined by field emission scanning electron microscope (SEM), the freeze dried gels were coated with approximately 10 nm of platinum using an Emitech K575X Peltier-cooled high resolution sputter coater (EM Technologies Ltd, Kent, England). These were viewed in a JEOL JSM-6700F SEM (JEOL Ltd, Tokyo, Japan).

2.3. Synthesis of mono (6-amino-6-deoxy)- β -CD, CD functionalized alginate and methacrylated gelatin

2.3.1. Mono (6-amino-6-deoxy)- β -CD or EDA- β -CD

EDA- β -CD was synthesized through a two-step reaction according to the reported procedure (Jalalvandi et al., 2016; Jalalvandi et al., 2017). First, a monotosyl derivative of β -CD was prepared by the reaction of *p*-toluene sulfonyl chloride with β -CD in water. Then, the product of first step was reacted with EDA at 80 °C in a sealed pressure tube for 8 h followed by precipitating into cold acetone. After filtration and drying under vacuum for 24 h, the product (EDA- β -CD) was collected as a white powder in 48% yield.

2.3.2. CD-functionalized alginate or CD-alginate

Alginate (1.0 g) was dissolved in distilled water (50 mL) and EDC (0.88 g, 4.5 mmol) as well as NHS (0.53 g, 4.5 mmol) were added to this solution. After an hour of stirring at room temperature, EDA- β -CD (1.64 g, 1.38 mmol) was added to the solution and reacted at room temperature for 24 h (Ji-sheng et al., 2016). The final solution was next placed in dialysis tubing for 48 h (Spectra/Por, MWCO 6000–8000 Da) and CD-alginate was collected after lyophilization in 1.33 g.

2.3.3. Methacrylated gelatin or Me-gelatin

Gelatin was modified following the previously reported procedure (Wouter et al., 2013). Briefly, methacrylic anhydride (1.0 g, 6.4 mmol) was added drop-wise to a solution of gelatin (1.0 g) in distill water (150 mL) at 50 °C. After 5 h, the solution was placed in a dialysis tubing and dialyzed against distill water for 48 h. Lyophilization yielded 0.92 g Me-gelatin.

Table 1

Precursors and their respective concentrations used in the preparation of hydrogels.

Composition of hydrogels	Shear thinning/self-healing hydrogel		Dual crosslinked hydrogel	
	Gel 1	Gel 2	Gel 3	Gel 4
CD-alginate (5 w/v%): Me-gelatin (10 w/v%)	1:1	2:1	1:1	2:1
Eosin Y-VP (μL)/ TEA (μL)	–	–	2.5 /5	2.5/5

2.4. Hydrogel preparation

The hydrogel precursors were prepared by dissolving CD-alginate (5 w/v%) and Me-gelatin (10 w/v%) in PBS. Table 1 shows the combination of these precursors used for preparation of each hydrogel. Gel 1 was made out of equal volume of CD-alginate and Me-gelatin solutions while gel 2 was prepared by mixing 2:1 ratio of the precursors. The precursors used for preparation of gel 3 and gel 4 contained photoinitiator and catalyst. Photosensitive initiator comprises of Eosin Y (1 mM, photo-sensitizer), TEA (125 mM, initiator), and VP (20 mM, catalyst). Note: The reported amount for photoinitiator and catalyst is for 1 mL of precursor mixture. To obtain the secondary crosslinked networks (gel 3 and gel 4), the precursors were mixed with the photoinitiator and first used to make the shear thinning materials (gel 1 and gel 2). Next, these shear thinning materials were then subjected to a visible green light illumination (525 nm).

2.5. In vitro hydrolytic degradation

Each hydrogel set ($n = 3$) was prepared in total volume of 1 mL and immersed in separate vials filled with PBS (30 mL). The vials were placed in incubator shaker (VWR® Incubating Orbital Shake) at 37 °C and the gels were removed in specific time intervals and lyophilized. Weight of each dry gel was recorded and compared with the initial weight of the dry gel at time = 0.

2.6. In vitro cytotoxicity

In vitro cell toxicity was conducted in 24-well plates (1 mL/well; BD Falcon) at a seeding density of 0.5×10^5 cells/mL using HMSC (passage 4) cell line. The hydrogel precursors were made in PBS and filtered (0.22 μm pore size, Millex GP) and placed in culture inserts (8 μm pore size, BD Falcon, USA) and mixed to produce the corresponding gel set

(0.5 mL). The precursors of gel 3 and gel 4 were then exposed to green light for 10 min to complete the secondary crosslinking process. These culture inserts were then immersed in culture wells pre-seeded with HMSC ($n = 3$ for each gel set). The same volume of 10% SDS (0.5 mL) and media were deposited in cultured inserts to serve as a positive and normal growth control respectively. Cell viability was determined after 24 h incubation for each hydrogel group compared to non-treated HMSC control cells using MTT assay. After 24 h, the culture inserts and media were removed and replaced by fresh media (200 μL). MTT solution (5 mg/mL, 20 μL) was added to each well and incubated for 3 h at 37 °C. After 3 h, MTT was removed and replaced by DMSO (250 μL) to dissolve the formed formazan in each well. The absorbance of each well was measured at 540 nm with a plate reader (Tecan group Ltd., Männedorf, Switzerland). The viability of cells in the presence of each gel was then calculated (Jalalvandi et al., 2016).

3. Results and discussion

3.1. Synthesis and characterization of precursors

EDA- β -CD was obtained by modification of β -CD to produce a primary amine substituent on the cyclodextrin cavity. The structure, ^1H NMR and FTIR spectra of EDA- β -CD are shown in Figs. 1 and 3, respectively. ^1H NMR (Fig. 1A): 5 (s, 7H), 3.93–3.62 (m, 28H), 3.6–3.4 (m, 14H), 2.85–2.65 (m, 4H). FTIR (neat, cm^{-1}): 3334 (m, OH, NH_2), 2927 (m, CH_2), 1660 (m, C-H stretching vibration of methyne groups) and 1151, 1024, (s, C-O-C stretching vibration) (Fig. 3). The results are in agreement with previously reported spectra (Jalalvandi et al., 2016; Jalalvandi et al., 2017).

The amine group on EDA- β -CD was then coupled with carboxylic functionalities of alginate via EDC coupling to form stable amide bonds. The first step of the EDC coupling mechanism was activation of a carboxylic acid group with EDC and NHS to form an active O-acylisourea intermediate. This intermediate directly reacted with the primary amine of EDA- β -CD to yield CD-alginate in the next step and the by-product was removed during dialysis process. It was initially found that CD-alginate with a high proportion (50 mol%) of EDA- β -CD had poor solubility. Hence, the amount of EDA- β -CD was kept lower at 30 mol% which was confirmed by ^1H NMR spectrum of CD-alginate (Fig. 1B). Fig. 1B shows the appearance of new peaks corresponding to the presence of CD in CD-alginate structure at 3 ppm and 5 ppm (compare to the spectrum of alginate alone, Fig. 1C). Also, FTIR spectrum of CD-alginate shows the presence of a new peak at around 1700 cm^{-1} which is attributed to the C=O stretching vibration of the secondary amide formed during EDC coupling (Ji-sheng et al., 2016).

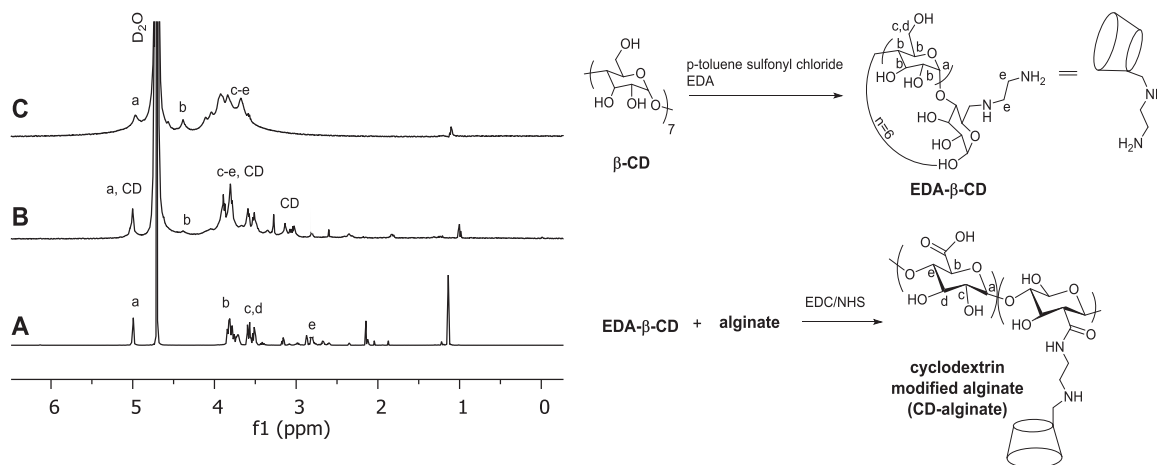


Fig. 1. Structure of EDA- β -CD and CD-alginate (right side). (A) ^1H NMR spectrum of EDA- β -CD. (B) ^1H NMR spectrum of CD-alginate. (C) ^1H NMR spectrum of alginate alone. All the spectra were obtained in D_2O as solvent and at 24.8 °C. The signals and their corresponding protons are labeled in the chemical structures and the spectra.

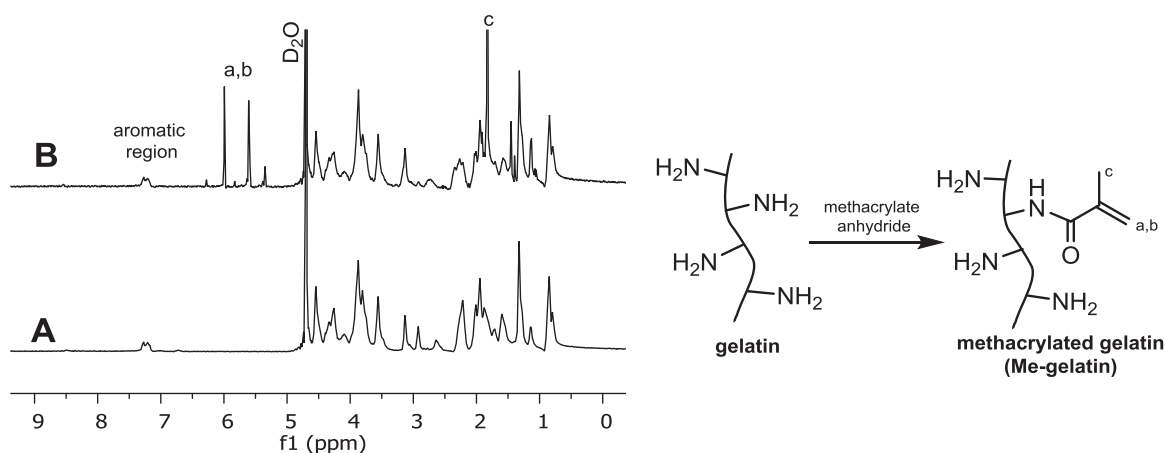


Fig. 2. Schematic structure of Me-gelatin and gelatin (right side). (A) ^1H NMR spectrum of gelatin alone (B) ^1H NMR spectrum of Me-gelatin. All the spectra were obtained in D_2O as solvent and at 24.8°C . The signals and their corresponding protons are labeled in the chemical structures and the spectra.

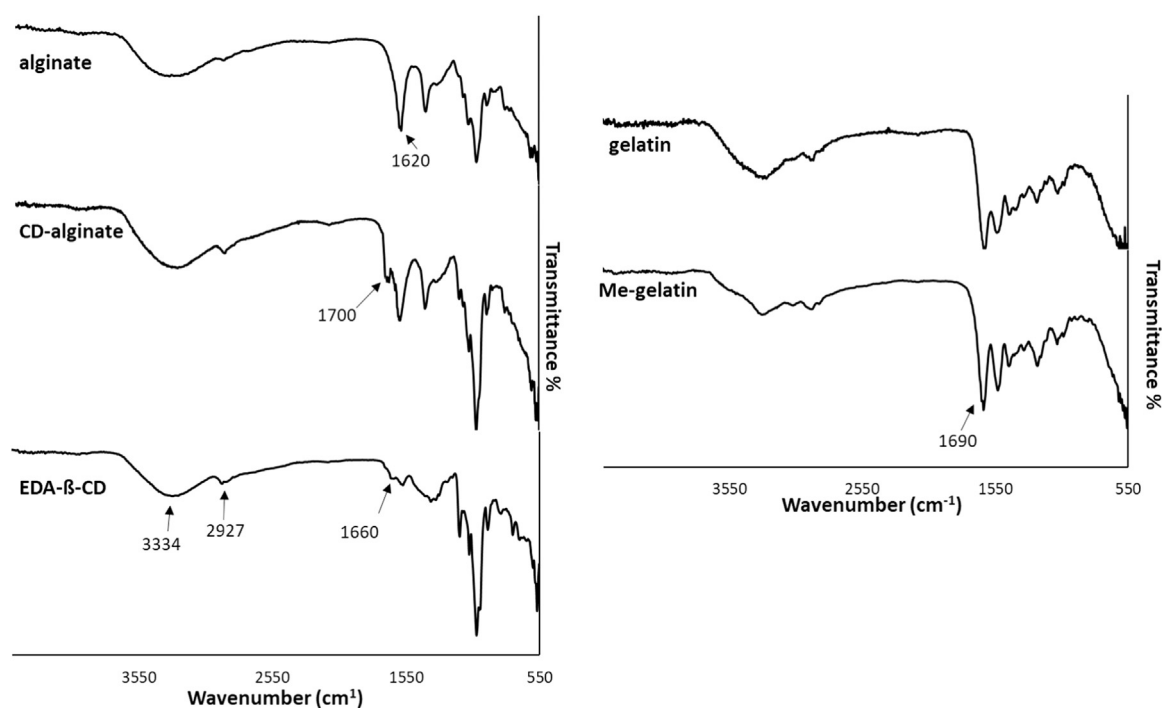


Fig. 3. FTIR spectra of alginate, EDA- β -CD, CD-alginate, gelatin and Me-gelatin.

To impart the photocrosslinkable functionalities in gelatin, methacrylic anhydride was used to react with primary amine groups of gelatin and produce amide linkages. In ^1H NMR spectrum of Me-gelatin (Fig. 2B), the presence of new signals representing vinyl group (5.5 and 6 ppm) as well as methyl group (1.82 ppm) confirms the methacrylation reaction of gelatin (compare to spectrum of gelatin alone, Fig. 2A). The degree of methacrylation was calculated to be 38 mol% from NMR studies. This was defined as the ratio of methacrylate groups to the free amine groups in gelatin prior to the methacrylation reaction, as previously described (Zhou et al., 2014; Ovsianikov et al., 2011). Fig. 3 also shows the FTIR spectra of Me-gelatin and gelatin. A strong peak at 1690 cm^{-1} corresponds to carbon double bond in MA-Ge. The band at 1570 cm^{-1} represents to C-N-H bending while the band at $3200\text{--}3400\text{ cm}^{-1}$ indicates the presence of peptide bonds (N-H stretching) (Rahali et al., 2017).

3.2. Rheological measurements

3.2.1. Viscosity

Viscosity of the precursors, CD-alginate (5 w/v%) and Me-gelatin (10 w/v%), without the presence of the photoinitiator was measured at shear rates ranging from 1 to 100 (1/s), over one-minute period at 25°C and 37°C . Since gelatin aqueous solution tends to solidify faster at lower temperature, two different temperatures (25°C and 37°C) were chosen to carry out the rheological analyses. Fig. 4 presents the viscosity values of the precursors. CD-alginate showed higher viscosity compared to Me-gelatin at both temperatures. The viscosity of Me-gelatin decreases with increasing temperature to 37°C . This observation agrees with previous reports (Tabata and Ikada, 1999; Davis et al., 1921). Gelatin dissolves in warm water, 37°C , and exist as random coils in aqueous solution which are unique entities moving freely in the solution, however, at lower temperature, 25°C , a transition occurs leading to formation of a thermos-reversible and physically crosslinked gel (Tabata and Ikada, 1999; Hayashi and Oh, 1983). Similar to Me-

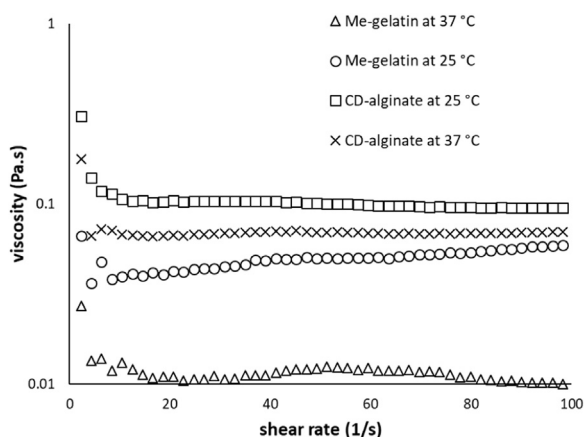


Fig. 4. Viscosity values of both precursors at 25 °C and 37 °C monitored for 60 s.

gelatin, CD-alginate showed lower viscosity value at 37 °C compared to 25 °C. Decrease in temperature results in the formation of crystallites CD (Szejtli, 1998). Since CD moieties are distributed into alginate backbone, a modest change of turbidity occurred which means higher viscosity values at 25 °C for CD-alginate (Burckbuchler et al., 2006). Overall, Fig. 4 suggests that CD-alginate is more viscous material compared to Me-gelatin at both temperatures. This might be due to different characteristics of these biopolymers such as molecular weight and intramolecular interactions (e.g., solvent-polymer).

3.2.2. Cyclic strain time sweep (Shear thinning/self-healing)

To test the self-healing and recovery properties of the materials, the shear thinning hydrogels (gel 1 and gel 2) were subjected to four cycles of low amplitude oscillatory strain (0.5%) followed by high amplitude oscillatory strain (250%) at 10 Hz and at 25 °C and 37 °C. (Note: oscillatory frequency sweeps were performed at 0.5% strain with an elevating frequency of 0.1–100 Hz during which, hydrogels demonstrated steady state behavior up to 10 Hz which was selected for strain sweep studies). The precursors of each gel were mixed and immediately formed the gels which were then analyzed through a cyclic deformation. The results of dynamic shear strain tests are shown in Fig. 5 where storage modulus, G' , response to changes in strain were monitored for gel 1 and 2 at 25 °C and 37 °C. This figure exhibits a sharp decrease in G' values for both hydrogels at high strain which were recovered instantly at low strains upon removal of shear. The ability of both gel 1 and gel 2 to recover from deformation (high strain, 250%) demonstrates their self-healing properties. The guest-host interaction between CD moieties in CD-alginate and aromatic region of Me-gelatin (e.g., tyrosine, phenylalanine, tryptophan) most likely drives the supramolecular assembly of physically crosslinked hydrogel (gel 1 and gel 2). Due to reversible nature of this crosslinking mechanism, gel 1 and gel 2 are dynamic and capable of shear-induced flow and quick recovery (Fig. 5). The highest recovery degree was observed for gel 2 at 25 °C and 37 °C with 81% and 82%, respectively. Whereas, the recovery degree for gel 1 at 25 °C and 37 °C was about 79% and 69%, correspondingly. This can be explained by the higher density of CD moieties available for complexation with aromatic region in Me-gelatin since gel 2 had higher ratio 2:1 of CD-alginate and Me-gelatin (see Table 1). The more host molecules (CD) available, the faster crosslinking is and as a result the hydrogel could recover faster with greater degree. The effect of temperature on recovery degree is not conclusive as the recovery degrees for gel 2 at 25 °C and 37 °C are close. Nevertheless, gel 1 at 37 °C exhibited lower recovery degree compared to this gel at 25 °C. This might be due to the characteristics of gelatin chains that could move freely at higher temperature and present as physically crosslinked gel at lower temperatures as discussed for viscosity results.

The guest-host interaction enables shear thinning/self-healing

characteristics of these gels. This physical interaction between CD and some aromatic moieties of gelatin such as tyrosine (Ma et al., 2015), phenylalanine (Aree et al., 2012) and tryptophan (Brown et al., 1994) has been investigated, previously. In the current study, tyrosine was chosen as a model aromatic moiety of gelatin and the formation of the inclusion complex between CD and tyrosine was investigated through ^1H NMR analysis (Fig. 6). L-tyrosine is not soluble in neutral water (pH 7.4), therefore, it was dissolved in a mixture of $\text{D}_2\text{O}/\text{DCl}$ to obtain its ^1H NMR spectrum. A mixture of L-tyrosine: EDA- β -CD or L-tyrosine: CD-alginate was prepared in D_2O and filtered to remove un-dissolved L-tyrosine. The solutions were then analyzed by ^1H NMR spectroscopy and the expansion of spectra in the aromatic region is illustrated in Fig. 6C. Clear shift in the signals of L-tyrosine in the presence of EDA- β -CD or CD-alginate proposed the formation of inclusion complex (Jalalvandi et al., 2016; Akita et al., 2014). The chemical shifts were similar in both L-tyrosine: EDA- β -CD and L-tyrosine: CD-alginate mixture suggesting the similar binding mechanism of tyrosine to CD. This proves that the aromatic region of Me-gelatin could interact with CD moieties of CD-alginate to form the physically crosslinked hydrogels, gel 1 and gel 2. The schematic mechanism of formation of the inclusion complex between the guest molecule (tyrosine) and the host molecule (CD) is shown in Fig. 6A and B (Shanmugam et al., 2008). Two different mechanisms for the formation of inclusion complexes are proposed in this figure. In the first method, the phenolic OH group of L-tyrosine is entrapped within the CD cavity and in the second method, the carboxyl group of L-tyrosine, $-\text{COOH}$, is captured in the CD cavity. Formation of an inclusion complex is a result of equilibrium between the guest molecule and the host molecule which is a reversible process (Layre et al., 2002). Steric and thermodynamic factors are involved in an inclusion complex formation. The driving forces for this phenomenon are attributed to the removal of water molecules from the hydrophobic cavity and formation of van der Waals interactions, release of CD ring strain, hydrophobic interactions and hydrogen bonding with CD's hydroxyl groups (Loftsson and Brewster, 1996; Mahedero et al., 2002). Overall, gel 1 and gel 2 were formed via a weak physical crosslinking process. This crosslinking was generated by a guest-host interaction between CD moieties of CD-alginate and aromatic moieties of Me-gelatin. This reversible physical interaction was used to create a hydrogel network with shear thinning and self-healing properties.

3.2.3. Strain sweep

To further confirm the shear thinning properties of these injectable hydrogels, the components of gel 1 and gel 2 were subjected to oscillatory strain sweeps from 0.1% to 500% radial strain at 10 Hz. The results are shown in Fig. 7 where storage modulus (G') and loss modulus (G'') of gel 1 and gel 2, crossed at high strain. The cross-over point marks a solid to liquid transition which happens due to the presence of low and high strain, respectively. At low strains, both gel 1 and gel 2, were more elastic with greater value of G' compared to G'' . For gel 1, the cross-over point appeared at around 10% strain or lower (at 25 °C) indicating a transition from an elastic solid material to a viscous liquid. However, the cross-over point began to form after 10% strain for gel 2 at both temperatures (25 °C and 37 °C) suggesting that the crosslinking density for gel 2 was greater than crosslinking density of gel 1.

3.2.4. Time sweep

To monitor the gelation kinetics of each hydrogel, oscillatory time sweep was performed at 10 Hz, 1% strain at 25 °C and 37 °C for gel 1 and gel 2 with single crosslinking method and for gel 2 and gel 3 with dual crosslinking technique.

3.2.5. Single crosslinking method (shear thinning materials)

CD-alginate and Me-gelatin formed gels almost immediately after mixing their corresponding precursors. To perform the time sweep experiment, the components of gel 1 or gel 2 were placed in two 5 mL syringes which were then connected with a Couple Luer Tapered. The

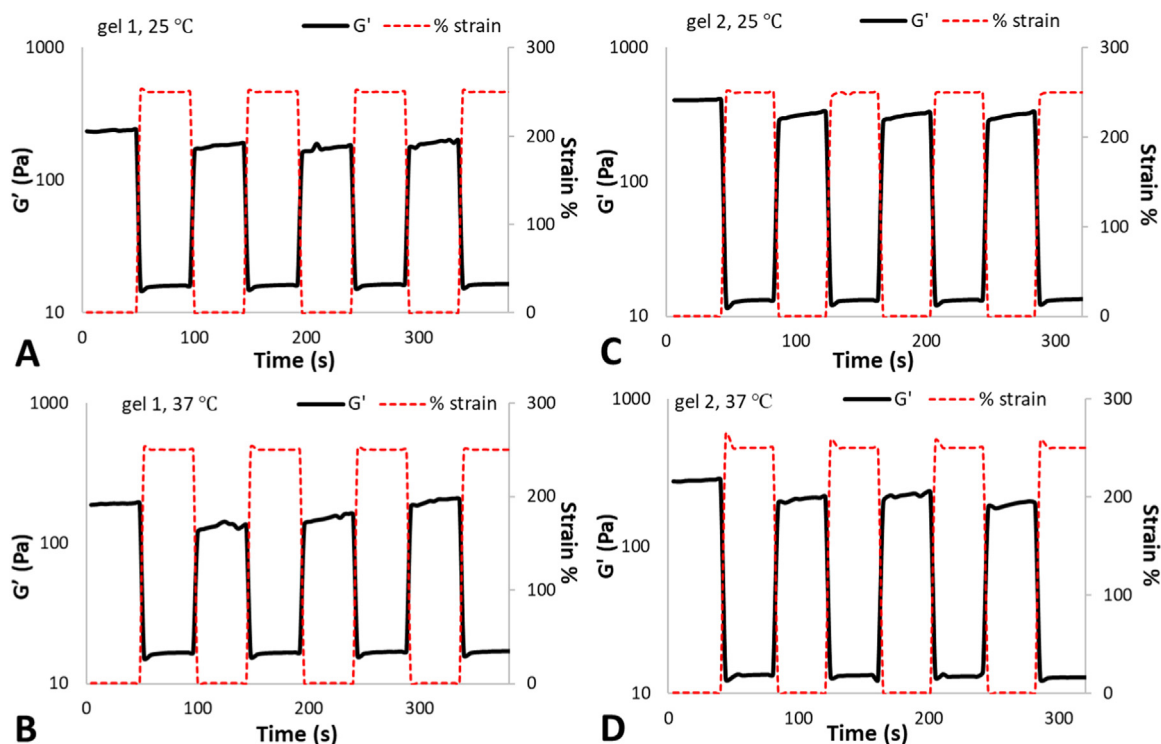


Fig. 5. (A–D) Corresponding recovery of gel 1 and gel 2 at 25 °C and 37 °C undergoing a cyclic deformation of 0.5% (low strain %) and 250% (high strain %) at 10 Hz (four cycles). The dynamic nature of physical guest-host interaction results in shear thinning characteristics of these hydrogels. Both gels undergo a disassembly when shear forces are applied (high strain %) and are self-healing once the shear forces are removed (low strain %).

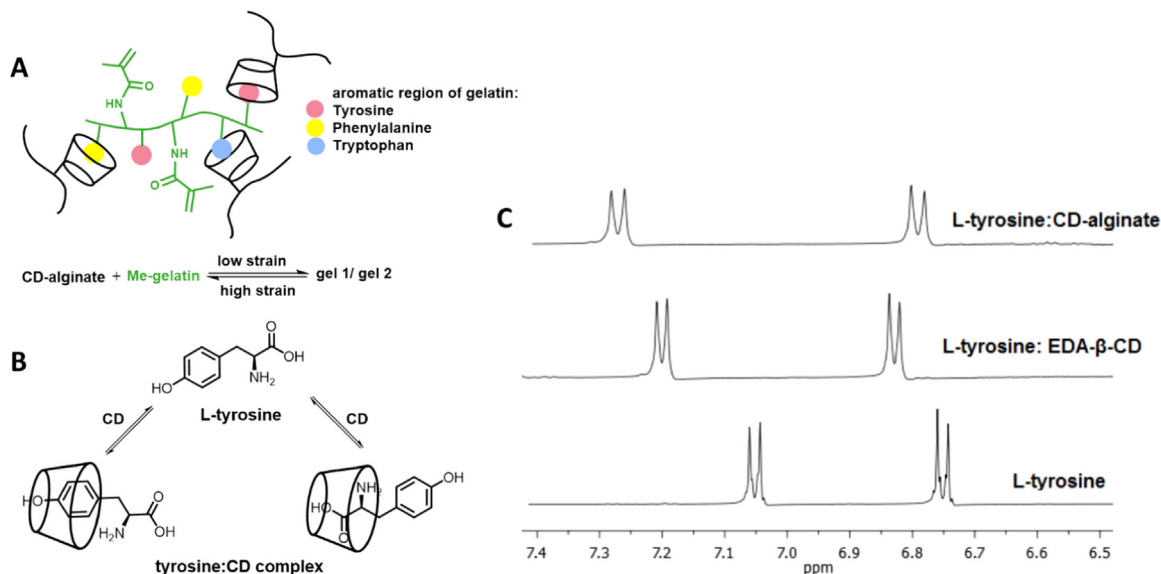


Fig. 6. (A) Complexation between CD moieties of CD-alginate (black polymer backbone) and aromatic region of Me-gelatin (green polymer backbone) drives the reversible crosslinking mechanism for gel 1 and gel 2. (B) Proposed encapsulation method for L-tyrosine. (C) Expansion of ^1H NMR spectra of L-tyrosine in $\text{D}_2\text{O}/\text{DCL}$, L-tyrosine:EDA- β -CD in D_2O and L-tyrosine:CD-alginate in D_2O .

components were mixed thoroughly and pushed into one of the syringes equipped with a 15-gauge needle. The sample (300 μL) was placed on the rheometer plate and storage G' and loss G'' modulus were measured as a function of time for 10 min at 25 °C and 37 °C. Fig. 8 shows the results of time sweep test for shear thinning materials, gel 1 and gel 2. Since gel 1 and gel 2 already were formed by mixing the precursors in the syringe, the G' values were higher than G'' from the beginning of test which suggests the formation of the hydrogels (Jalalvandi et al., 2016). G' and G'' values remained plateau throughout the experiment

showing the stable state of the hydrogels where no further crosslinking occurred. The G' values for gel 2 were slightly higher compared to gel 1 at the two different tested temperatures. This might be due to the higher amount of CD-alginate in gel 2 compared to gel 1 (see Table 1 for precursor ratio) which resulted in more crosslinking density and, subsequently higher storage modulus.

3.2.6. Secondary crosslinking method (dual crosslinked network)

The precursors of gel 2 and gel 3 were prepared according to Table 1

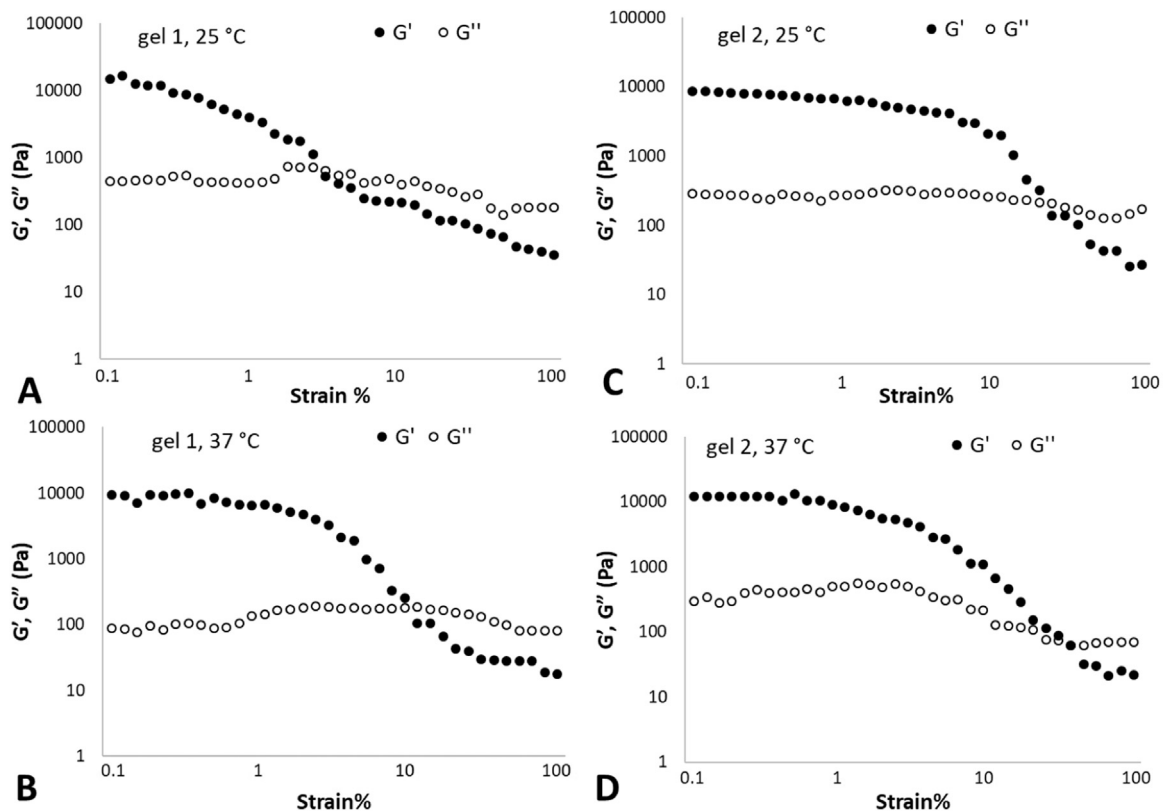


Fig. 7. Oscillatory strain sweeps were performed on the components of gel 1 and gel 2 without photocrosslinking reagent at 25 °C and 37 °C at 10 Hz using strain% from 0.1% to 500%.

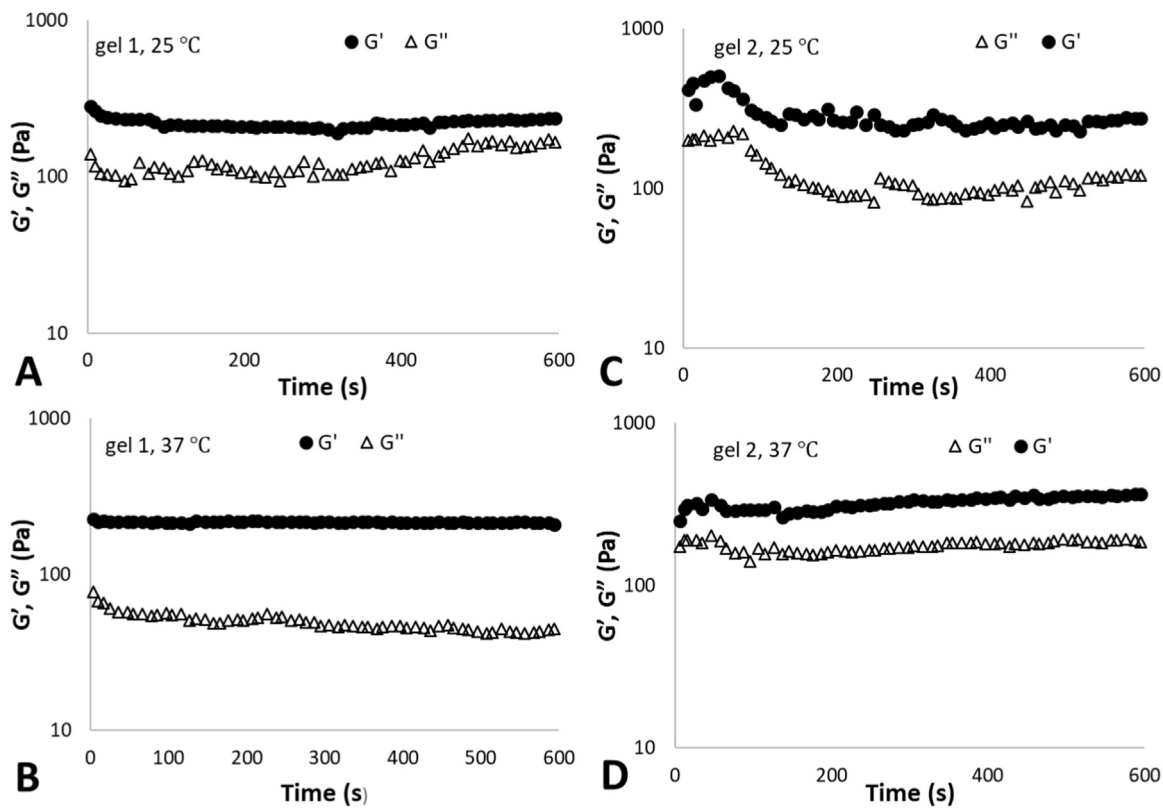


Fig. 8. Time sweep test on the components of gel 1 and gel 2 without photocrosslinking at 25 °C and 37 °C for a 10 min period. In all tests G' values are higher than G'' values suggesting a solid state.

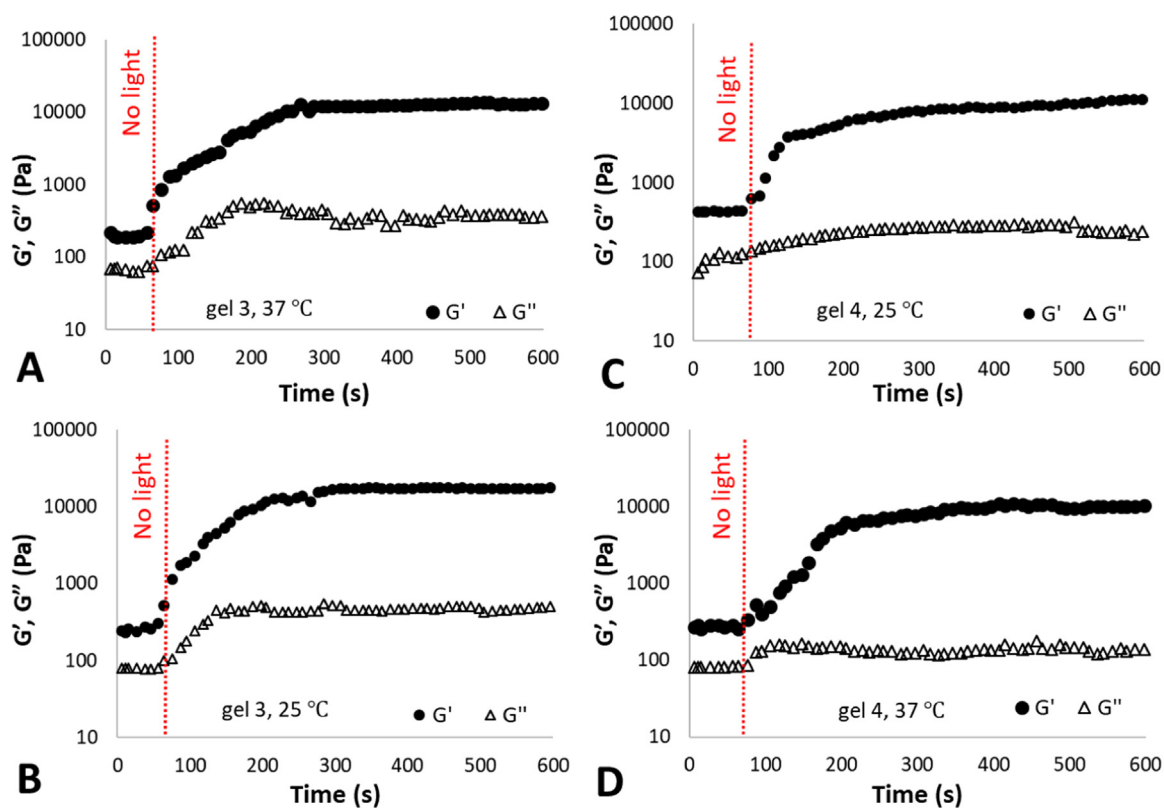


Fig. 9. Time sweep of photocrosslinking with visible light exposure to produce gel 3 and gel 4 at 25 °C and 37 °C, 1 Hz. The red line represents the border between single crosslinked network (gel 1 and gel 2) and dual crosslinked matrices after green light illumination (gel 3 and gel 4).

(containing photoinitiator) and they were placed on the rheometer plate using a 5 mL syringes equipped with a 15-gauge needle under red light. Exposure of these components containing photoinitiator to the red light is not risky, as the photoinitiator is not activated in this wavelength (635–700 nm). This step resulted in the formation of shear thinning material which is shown as a lower step in Fig. 9 on the left side of the graphs (no secondary crosslinking occurred). Due to the presence of photocrosslinkable vinyl functionalities on Me-gelatin, these gels could undergo a secondary covalent crosslinking process in the presence of the photoinitiator (Eosin Y-VP/TEA). Exposure to visible green light (525 nm) initiates radical polymerization resulting in a significant increase in storage modulus values (Fig. 9 right side of the graphs). Gel 3 and gel 4 were produced through a dual crosslinking process including a physical crosslinking via a guest-host interaction (resulted in gel 1 and gel 2) followed by a chemical crosslinking technique using photocrosslinkable functional groups. The highest G' value was associate to gel 3 at 25 °C (~17,000 Pa). This was expected knowing the higher ratio of Me-gelatin in this gel compared to gel 4. Owing the high concentration of Me-gelatin, the higher crosslinking density and stiffer network was achieved after photocrosslinking the vinyl groups of Me-gelatin for gel 3. The lowest value of storage modulus was observed for gel 4 at 37 °C (~8500 Pa) which contained lower amount of Me-gelatin responsible for secondary crosslinking and increase in G' values. The effect of temperature was not significant, however, lower temperature led to higher G' value as discussed previously, in Section 3.2.1, viscosity.

Generally, the results from strain sweep (Fig. 5) and time sweep studies (Fig. 8) for gel and gel 2 showed the formation of hydrogels with shear thinning/self-healing properties. Since these hydrogels were formed via a weak physical crosslinking process, they showed weak mechanical properties. It was hypothesized that a chemically cross-linked hydrogel is more stable than a physically crosslinked hydrogel and shows stronger mechanical properties. To investigate the effect of a

chemical crosslinking process on the mechanical properties of the hydrogels, a secondary crosslinking mechanism was introduced to these systems to further crosslink gel 1 and gel 2 and prepare more stable networks as gel 3 and gel 4 (see time sweep experiment for gel 3 and gel 4). These dual crosslinked hydrogels were no longer shear thinning as they formed more stable networks via photocrosslinking compared to gel 1 and gel 2. The results from time sweep experiments (Figs. 8 and 9) confirmed the hypothesis when dual crosslinked networks, gel 3 and gel 4, showed higher value of G' compared to gel 1 and gel 2. This suggests stiffer network for gel 3 and gel 4 compared to gel 1 and gel 2 due to the higher amount of crosslinking density (generated by two different crosslinking mechanisms) in these dual crosslinked matrices.

3.3. Degradation study

The results of hydrolytic degradation are presented in Fig. 10. Shear

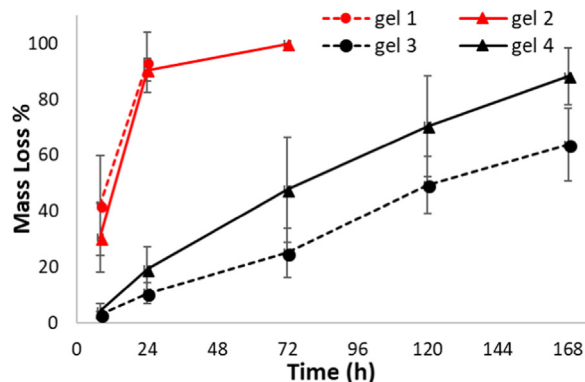


Fig. 10. Hydrolytic degradation of shear thinning hydrogels (gel 1 and gel 2) and dual crosslinked networks (gel 3 and gel 4) at 37 °C in PBS (pH 7.4).

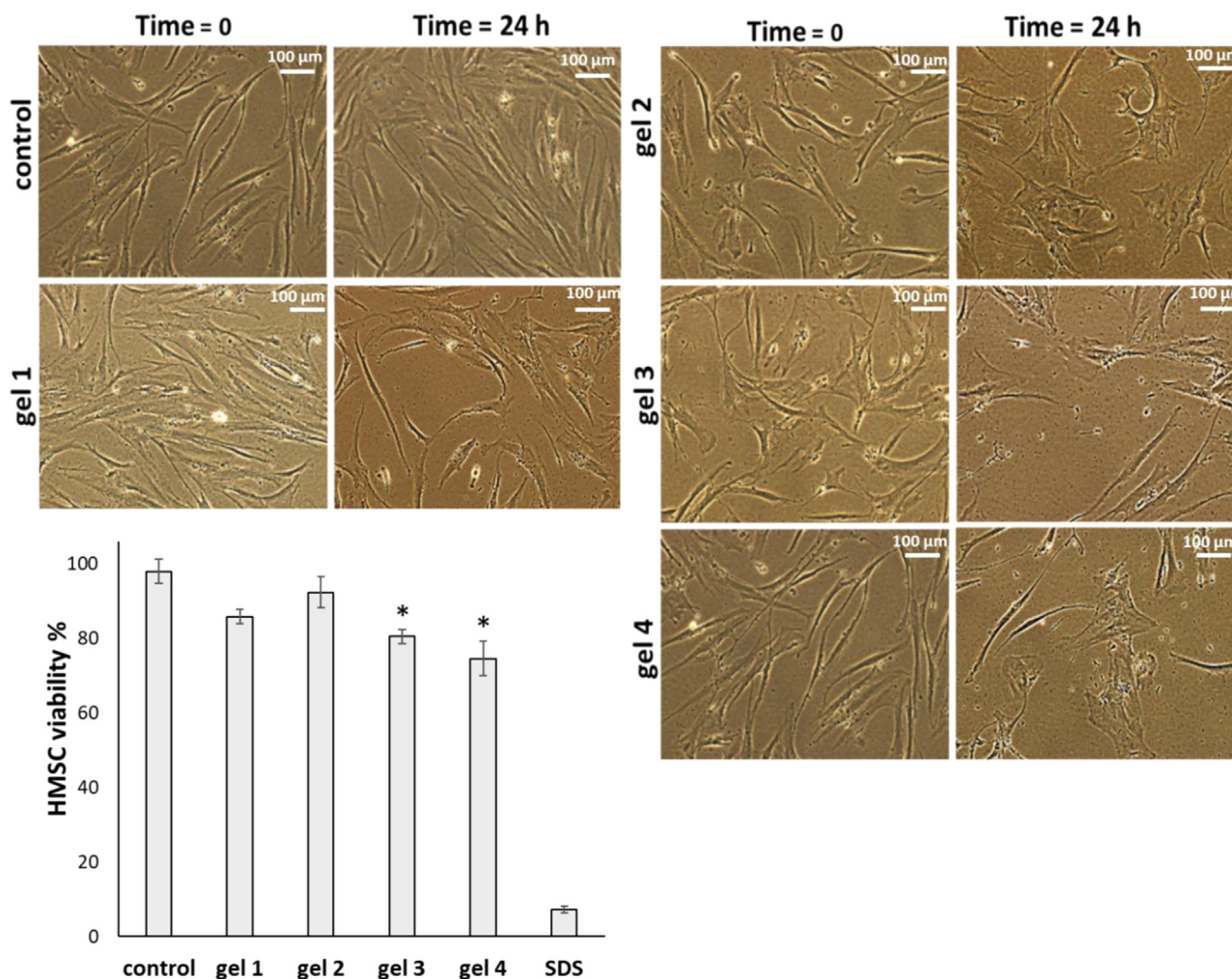


Fig. 11. Representative images of HMSC cells after culturing for 24 h and before exposing to hydrogels (time = 0), after exposing to hydrogels for 24 h (time 24 h). scale bar is presented beside the representative images. The results of cell viability studies using MTT assay are shown in the graph where the statistical significance was set at $*p \leq 0.05$. Data are reported as mean \pm standard deviation ($n = 3$). The results were statistically analyzed by one-way analysis of variance (ANOVA) with Bonferroni post-test. HMSC cells showed more than 74.5% viability when exposed to the hydrogels for 24 h at 37 °C, 5% CO₂.

thinning/self-healing hydrogels (gel 1 and gel 2) are based on inherently weak physical crosslinking method (guest-host interactions) as opposed to stable covalent crosslinking technique (photocrosslinking). This can lead to fast degradation rates and dissolution in as short as hours. Gel 1 completely degraded in 24 h in PBS which proves the weak guest-host interaction employed for formation of this hydrogel. Whereas, gel 3 demonstrated the slowest degradation rate due to the highest crosslinking density generated by two methods of crosslinking including physical interaction followed by photocrosslinking. Secondary crosslinking through a chemical reaction created a more stable network for gel 3 and gel 4 compared to unstable gel 1 and gel 2. This was also confirmed by rheological analyses and the time sweep experiment results. It is worth mentioning the same pattern of degradation for gel 1 and gel 2 as well as gel 3 and gel 4 suggesting similar crosslinking techniques used for their preparation.

3.4. Biocompatibility test

To assess the biocompatibility of these hydrogels and their potential degradation products in 24 h period, the viability of HMSC cells were studied in the presence of all the hydrogels according to International Organization for Standardization, Part 5: Tests for in vitro cytotoxicity of medical devices (ISO 10993–5:2009) (Jalalvandi et al., 2018; Srivastava et al., 2018). This is an indirect contact test that allows for

the interaction of any leachable byproduct with the cell monolayer. In this method, the material (hydrogel) is placed into a transwell insert, which is cultured with HMSC seeded on the bottom of the well plate. HMSC showed about 86%, 92%, 80.5% and 74% viability after 24 exposure to the gel 1, gel 2, gel 3 and gel 4, respectively (Fig. 11). The cell viability was lower in the presence of gel 3 and gel 4 compared to gel 1 and gel 2. The less viability in the presence of the dual crosslinked hydrogels could be associated with the use of photoinitiator/catalyst in the crosslinking process and the cytotoxic effect of photoinitiator system on HMSC cell line.

3.5. Morphology of hydrogels

The SEM images of all hydrogels are presented in Fig. 12. The freeze dried hydrogels clearly exhibited the presence of porous structures which somewhat are artefacts of the drying process. However, the morphological pattern of gel 1 is similar to gel 2 and also SEM image of gel 3 is similar to gel 4. This might be due to the same crosslinking process used for preparation of these gels.

4. Conclusion

The most common strategy to produce injectable hydrogels is to develop a system that can easily be injected as a low viscosity liquid

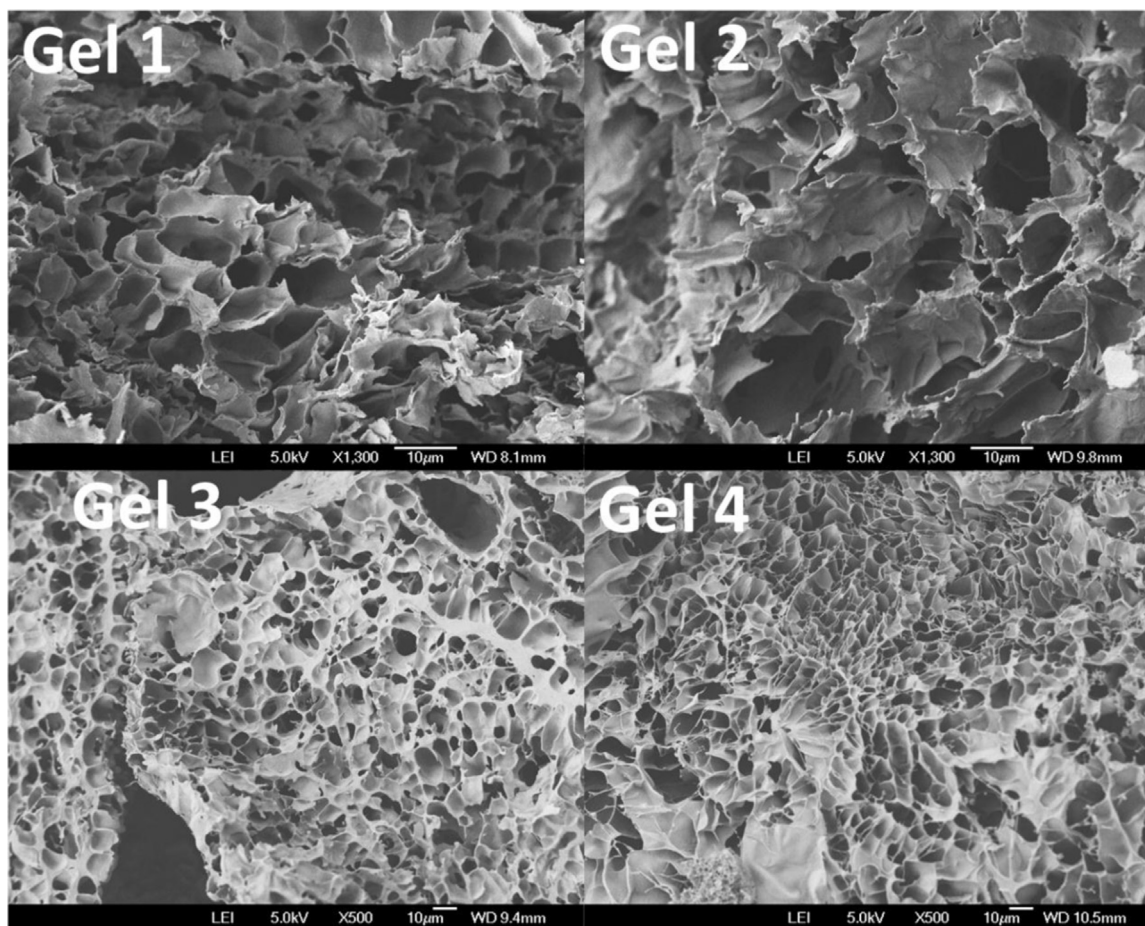


Fig. 12. SEM images of gel 1, gel 2 (up), gel 3 and gel 4 (down) operating at 5 kV.

followed by formation of a solid phase network. In this work, a shear thinning/self-healing hydrogel was synthesized which was then further crosslinked by a covalent photocrosslinking method. The self-healing properties of this system was generated by the formation of inclusion complex between hydrophobic cavity of cyclodextrin attached to alginate backbone and aromatic region of gelatin. The secondary crosslinking was carried out by the radical photopolymerization of methacrylated gelatin in the presence of a photoinitiator by visible green light illumination. The rheological analyses confirmed the recovery ability of the shear thinning material. Also, the gelation kinetic for secondary crosslinking method was studied where the networks formed showed significantly higher storage modulus compared to physically cross-linked shear thinning hydrogels. These hydrogels are based on biopolymers which are degradable and demonstrated no significant toxicity towards HMSC cell line. These matrices have the potential to be used in tissue engineering and cell or drug delivery. However, for future studies, a more in depth cytotoxicity test with relevant cell type to a specific application as well as use of a range of needle-sizes are recommended.

Acknowledgement

The authors would like to thank the help of Otago University and the University of Vermont. This study did not receive any specific funding.

References

Akita, T., Matsui, Y., Yamamoto, T., 2014. A ¹H NMR titration study on the binding constants for D- and L-tryptophan inclusion complexes with 6-O- α -D-glucosyl- β -

cyclodextrin. Formation of 1:1 and 2:1 (host:guest) complexes. *J. Mol. Struct.* 1060, 138–141.

- Appel, E.A., del Barrio, J., Loh, X.J., Scherman, O.A., 2012. Supramolecular polymeric hydrogels. *Chem. Soc. Rev.* 41, 6195–6214.
- Appel, E.A., Forster, R.A., Rowland, M.J., Scherman, O.A., 2014. The control of cargo release from physically crosslinked hydrogels by crosslink dynamics. *Biomaterials* 35, 9897–9903.
- Aree, T., Arunchai, R., Koonruga, N., Intasiri, A., 2012. Fluorometric and theoretical studies on inclusion complexes of β -cyclodextrin and D-, L-phenylalanine. *Spectrochim. Acta Part A: Mol. Biomol. Spectrosc.* 96, 736–743.
- Arya, A.D., Hallur, P.M., Karkisaval, A.G., et al., 2016. Gelatin methacrylate hydrogels as biomimetic three-dimensional matrixes for modeling breast cancer invasion and chemoresponse in vitro. *ACS Appl. Mater. Interfaces* 8, 22005–22017.
- Baroli, B., 2006. Photopolymerization of biomaterials: issues and potentialities in drug delivery, tissue engineering, and cell encapsulation applications. *Chem. Technol. Biotechnol.* 81, 491–499.
- Brown, S.E., Coates, J.H., Easton, C.J., et al., 1994. Tryptophan anion complexes of β -cyclodextrin (cyclomaltaheptaose), an aminopropylamino- β -cyclodextrin and its enantioselective nickel(II) complex. *J. Chem. Soc., Chem. Commun.* 47.
- Bryant, S.J., Nuttelman, C.R., Anseth, K.S., 2000. Cytocompatibility of UV and visible light photoinitiating systems on cultured NIH/3T3 fibroblasts in vitro. *Biomater. Sci. Polym. Ed.* 11, 439–457.
- Burckbuchler, V., Kjøniksen, A.-L., Galant, C., et al., 2006. Rheological and structural characterization of the interactions between cyclodextrin compounds and hydrophobically modified alginate. *Biomacromolecules* 7, 1871–1878.
- Chhatbar, M.U., Prasad, K., Chejara, D.R., Siddhanta, A.K., 2012. Synthesis of sodium alginate based sprayable new soft gel system. *Soft Matter* 8, 1837–1844.
- Dankers, P.Y.W., Hermans, T.M., Baughman, T.W., Kamikawa, Y., Kieltyka, R.E., Bastings, M.M.C., Janssen, H.M., Sommerdijk, N.A.J.M., Larsen, A., van Luyn, M.J.A., Bosman, A.W., Popa, E.R., Fytas, G., Meijer, E.W., 2012. Hierarchical formation of supramolecular transient networks in water: a modular injectable delivery system. *Adv. Mater.* 24, 2703–2709.
- Davis, C.E., Oakes, E.T., Browne, H.H., 1921. Viscosity of gelatin solutions. *J. Am. Chem. Soc.* 43, 1526–1538.
- Ding, X., Gao, J., Awada, H., Wang, Y., 2016. Dual physical dynamic bond-based injectable and biodegradable hydrogel for tissue regeneration. *J. Mater. Chem. B* 4, 1175–1185.
- Duconseille, A., Astruc, T., Quintana, N., Meersman, F., Sante-Lhoutellier, V., 2015. Gelatin structure and composition linked to hard capsule dissolution: a review. *Food*

- Hydrocoll. 43, 360–376.
- Farris, S., Song, J., Huang, Q., 2010. Alternative Reaction Mechanism for the Cross-Linking of Gelatin with Glutaraldehyde. *J. Agric. Food Chem.* 58, 998–1003.
- Fedorovich, N.E., Oudshoorn, M.H., van Geemen, D., Hennink, W.E., Alblas, J., Dhert, W.J., 2009. The effect of photopolymerization on stem cells embedded in hydrogels. *Biomaterials* 30, 344–353.
- Feng, Q., Wei, K., Lin, S., et al., 2016. Mechanically resilient, injectable, and bioadhesive supramolecular gelatin hydrogels crosslinked by weak host-guest interactions assist cell infiltration and in situ tissue regeneration. *Biomaterials* 101, 217–228.
- Guvendiren, M., Lu, H.D., Burdick, J.A., 2012. Shear-thinning hydrogels for biomedical applications. *Soft Matter* 8, 260–272.
- Hao, Y., Shih, H., Muñoz, Z., Kemp, A., Lin, C.-C., 2014. Visible light cured thiol-vinyl hydrogels with tunable degradation for 3D cell culture. *Acta Biomater.* 10, 104–114.
- Hayashi, A., Oh, S.-C., 1983. Gelation of gelatin solution. *Agric. Biol. Chem.* 47, 1711–1716.
- Huang, G., Li, F., Zhao, X., et al., 2017. Functional and biomimetic materials for engineering of the three-dimensional cell microenvironment. *Chem. Rev.* 117, 12764–12850.
- Jalalvandi, E., Cabral, J., Hanton, L.R., Moratti, S.C., 2016. Cyclodextrin-polyhydrazine degradable gels for hydrophobic drug delivery. *Mater. Sci. Eng.: C* 69, 144–153.
- Jalalvandi, E., Hanton, L.R., Moratti, S.C., 2017. Schiff-base based hydrogels as degradable platforms for hydrophobic drug delivery. *Eur. Polym. J.* 90, 13–24.
- Jalalvandi, E., Hanton, L.R., Moratti, S.C., 2018. Preparation of a pH sensitive hydrogel based on dextran and polyhydrazide for release of 5-fluorouracil, an anticancer drug. *J. Drug Deliv. Sci. Technol.* 44, 146–152.
- Ji-sheng, Y., Su-ya, H., Li, Y., Hai-cheng, Z., 2016. Synthesis of beta-cyclodextrin-grafted-alginate and its application for removing methylene blue from water solution. *J. Chem. Technol. Biotechnol.* 91, 618–623.
- Kim, G., Ahn, S., Kim, Y., Cho, Y., Chun, W., 2011. Coaxial structured collagen-alginate scaffolds: fabrication, physical properties, and biomedical application for skin tissue regeneration. *J. Mater. Chem.* 21, 6165–6172.
- Layre, A., Gosselet, N., Renard, E., Sebille, B., Amiel, C., 2002. Comparison of the Complexation of cosmetic and pharmaceutical compounds with γ -cyclodextrin, 2-hydroxypropyl- β -cyclodextrin and water-soluble β -cyclodextrin-co-epichlorhydrin polymers. *Incl. Phenom. Macrocycl. Chem.* 43, 311–317.
- Lee, F., Chung, J.E., Kurisawa, M., 2009. An injectable hyaluronic acid-tyramine hydrogel system for protein delivery. *J. Control. Release* 134, 186–193.
- Liu, L., Guo, Q.-X., 2002. The driving forces in the inclusion complexation of cyclodextrins. *J. Incl. Phenom. Macrocycl. Chem.* 42, 1–14.
- Loebel, C., Rodell, C.B., Chen, M.H., Burdick, J.A., 2017. Shear-thinning and self-healing hydrogels as injectable therapeutics and for 3D-printing. *Nat. Protoc.* 12, 1521–1541.
- Loftsson, T., Brewster, M.E., 1996. Pharmaceutical applications of cyclodextrins. 1. Drug solubilization and stabilization. *Pharm. Sci.* 85, 1017–1025.
- Lu, H.D., Soranno, D.E., Rodell, C.B., Kim, L.L., Burdick, J.A., 2013. Secondary photocrosslinking of injectable shear-thinning dock-and-lock hydrogels. *Adv. Healthc. Mater.* 2, 1028–1036.
- Ma, Y., Ji, Y., Zhong, T., et al., 2017. Bioprinting-based PDLSC-ECM screening for in vivo repair of alveolar bone defect using cell-laden, injectable and hotocrosslinkable hydrogels. *ACS Biomater. Sci. Eng.* 3, 3534–3545.
- Ma, M., Xu, S., Xing, P., Li, S., Chu, X., Hao, A., 2015. A multistimuli-responsive supramolecular vesicle constructed by cyclodextrins and tyrosine. *Colloid Polym. Sci.* 293, 891–900.
- Mahedero, M., De La Peña, A.M., Bautista, A., Aaron, J., 2002. An investigation of inclusion complexes of cyclodextrins with phenylurea herbicides by photochemically induced fluorescence. *analytical applications. Incl. Phenom. Macrocycl. Chem.* 42, 61–70.
- Manjula, B., Varaprasad, K., Sadiku, R., Raju, K.M., 2013. Preparation and characterization of sodium alginate-based hydrogels and their in vitro release studies. *Adv. Polym. Technol.* 32.
- Ovsianikov, A., Deiwick, A., Van Vlierberghe, S., et al., 2011. Laser fabrication of three-dimensional CAD scaffolds from photosensitive gelatin for applications in tissue engineering. *Biomacromolecules* 12, 851–858.
- Qiang, C., Lin, Z., Hong, C., et al., 2015. A novel design strategy for fully physically linked double network hydrogels with tough, fatigue resistant, and Self-healing properties. *Adv. Funct. Mater.* 25, 1598–1607.
- Qin, Z., Qu, B., Yuan, L., et al., 2017. Injectable shear-thinning hydrogels with enhanced strength and temperature stability based on polyhedral oligomeric silsesquioxane end-group aggregation. *Polym. Chem.* 8, 1607–1610.
- Rahali, K., Ben Messaoud, G., Kahn, C.J.F., et al., 2017. Synthesis and characterization of nanofunctionalized gelatin methacrylate hydrogels. *Int. J. Mol. Sci.* 18.
- Rodell, C.B., MacArthur Jr, J.W., Dorsey, S.M., Wade, R.J., Wang, L.L., Woo, Y.J., Burdick, J.A., et al., 2015. Shear-thinning supramolecular hydrogels with secondary autonomous covalent crosslinking to modulate viscoelastic properties in vivo. *Adv. Funct. Mater.* 25, 636–644.
- Schexneider, K.I., 2004. Fibrin sealants in surgical or traumatic hemorrhage. *Curr. Opin. Hematol.* 11, 323–326.
- Shanmugam, M., Ramesh, D., Nagalakshmi, V., Kavitha, R., Rajamohan, R., Stalin, T., 2008. Host-guest interaction of α -tyrosine with β -cyclodextrin. *Spectrochim. Acta Part A: Mol. Biomol. Spectrosc.* 71, 125–132.
- Srivastava, G.K., Alonso-Alonso, M.L., Fernandez-Bueno, I., et al., 2018. Comparison between direct contact and extract exposure methods for PFO cytotoxicity evaluation. *Sci. Rep.* 8, 1425.
- Su, K., Wang, C., 2015. Recent advances in the use of gelatin in biomedical research. *Biotechnol. Lett.* 37, 2139–2145.
- Szejtli, J., 1998. Introduction and general overview of cyclodextrin chemistry. *Chem. Rev.* 98, 1743–1754.
- Szekalska, M., Puciłowska, A., Szymańska, E., Ciosek, P., Winnicka, K., 2016. Alginate: current use and future perspectives in pharmaceutical and biomedical applications. *Int. J. Polym. Sci.* 2016, 17.
- Tabata, Y., Ikada, Y., 1999. Vascularization effect of basic fibroblast growth factor released from gelatin hydrogels with different biodegradabilities. *Biomaterials* 20, 2169–2175.
- Teodorescu, M., Andrei, M., Turturică, G., Stănescu, P.O., Zaharia, A., Sârbu, A., 2015. Novel thermoreversible injectable hydrogel formulations based on sodium alginate and Poly(N-Isopropylacrylamide). *Int. J. Polym. Mater. Polym. Biomater.* 64, 763–771.
- Wang, Z., Tian, Z., Menard, F., Kim, K., 2017. Comparative study of gelatin methacrylate hydrogels from different sources for biofabrication applications. *Biofabrication* 9, 044101.
- Wouter, S., LP, A., PM, W., et al., 2013. Gelatin-methacrylamide hydrogels as potential biomaterials for fabrication of tissue-engineered cartilage constructs. *Macromol. Biosci.* 13, 551–561.
- Yan, C., Altunbas, A., Yucel, T., Nagarkar, R.P., Schneider, J.P., Pochan, D.J., 2010. Injectible solid hydrogel: mechanism of shear-thinning and immediate recovery of injectable β -hairpin peptide hydrogels. *Soft Matter* 6, 5143–5156.
- Zhou, L., Tan, G., Tan, Y., Wang, H., Liao, J., Ning, C., 2014. Biomimetic mineralization of anionic gelatin hydrogels: effect of degree of methacrylation. *RSC Adv.* 4, 21997–22008.